Table IV: C-band Display and Recording Systems.

DISPLAY SYSTEMS	
HARDCOPY	VIDEO DISPLAY
• dry silver	• CRT monitor
• ~2000 pixels/line	• 512 pixels/line
• full header annotation	• full header annotation
• time & position blocks	• time & position blocks
• 16 grey levels	• 255 grey levels
• full or half narrow swath	• zoom to 2/1, 1/1, 1/2, 1/4 or 1/8
• full, 1/2, or 1/4 wide swath	• histogram display of full and/or zoom
• several display LUT's	• linear stretch or histogram equalization
• Edo Western	• Knudsen Engineering

RECORDING SYSTEMS		
SIGNAL	IMAGE	VIDEO
• 14-track HDDT	• 14-track HDDT	• video cassette
• all tracks used	• 5 tracks	
• variable speed	• 30 ips*	
• PCM coding	• PCM coding	• NTSC format
• 4096 range cells	• 4096 range cells	• 512 range cells
• time and Nav tagged	• time tagged	• time tagged
• range compressed	• fully compressed	• fully compressed
• 8-bits I and Q	• 8-bits amplitude	
• Bell and Howell	• Bell and Howell	

*To be increased in January, 1988 to 37.5 ips.

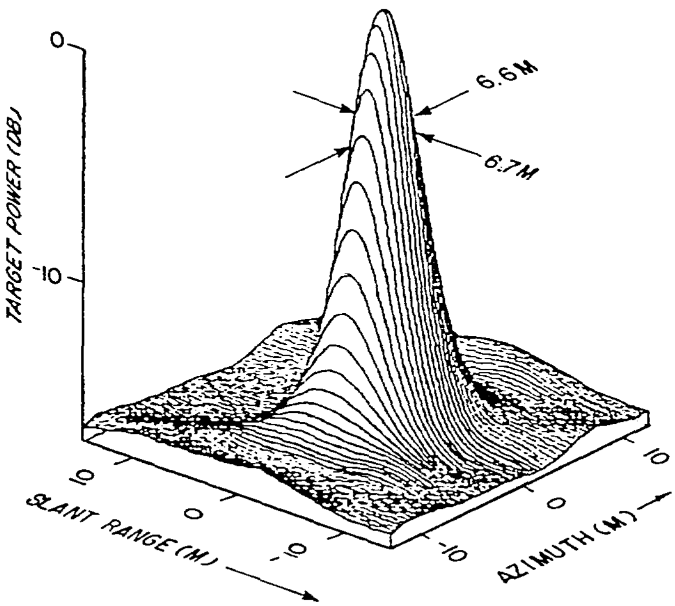

Figure 6: RTSP Impulse Response Function.
The 3-dimensional impulse response shown was taken from a nadir-mode RSTP image acquired on May 8, 1987. A point target was selected and the function generated by interpolating the radar response from a 8x8 pixel subimage around the point target. The full widths of the distribution at the 3 dB point are indicated.

Table V: Impulse Response Measurements from RTSP Imagery.

RADAR MODE	RESOLUTION Azimuth (m)	RESOLUTION Range (m)	INCIDENCE ANGLE (degrees)	TARGET RANGE (km)
Nadir	6.6	6.7	72.3	20.0
Narrow Swath	6.1	4.9	54.7	10.6
Wide Swath	9.5	18.9	79.9	34.7

σ_o by approximately 3 dB. These values are excellent. A 10 dB SNR will be obtainable even for cross-polarized narrow swath investigations of weakly scattering areas.

The high transmitter power is somewhat unusual. This is to satisfy the design goal to produce a flexible, research radar that could be used, for example, at shallow grazing angles over water and for quantitative research into cross-polarized signatures. Further, in the nadir mode, the angular range over which good data are required is $\sim 70^o$ and is much wider than the antenna elevation pattern. Again the high transmitted power allows us to use the STC to meet the very difficult design goal of imaging, *e.g.* the ocean, over a wide incidence angle range.

Some data acquired over marginal sea ice during the LIMEX experiment [1] have confirmed the potential of the radar for low backscatter research. When using a low power transmitter mode (test) with a peak transmitter output power of 0.4 kW (-20 dB from the nominal), narrow swath SNR's of 6-7 dB and 9-10 dB were obtained for far and mid-swath respectively. By extrapolating our C-band scatterometer results (measurements 10^o from to 60^o) to the far swath incidence angle ($\sim 74^o$) and comparing with backscatter data over this ice type, the probable σ_o at HH-polarization is -15 to -20 dB. These preliminary results yield a *noise equivalent* σ_o at full power to be in the -41 to -47 dB range. As there is a slight enhancement of the image SNR in relation to the receiver SNR for this radar [13] these values confirm the excellent performance for low backscatter scenes.

3.3 Geometric Fidelity

The on-board real-time processor sends data as indicated in Fig. 5 to a dry silver image recorder and to HDDT. This section is concerned with the geometric fidelity of these raw image outputs.

The dry silver product is automatically scaled and annotated to preserve the proper aspect ratio. Measurements from this output show that aspect ratio, averaged from 25 km section imagery, is correct to within 0.5%. In the recorded data stream, the aspect ratio is not unity as indicated in Table VI because the data are sampled at different rates in range and azimuth. The resolutions may also be different in these dimensions.

There are a number of reasons that the raw real-time processor imagery should have geometric distortions beyond those related to pixel sampling. The errors inherent in the RTSP products are small, but should be considered. Typical performance is listed in Table VII. The sources of error include: terrain elevation; azimuth processing skew; and in addition, small amounts of uncompensated motion or bias related to IRU or antenna pointing or moving scatterers within the scene.

Estimates can be made of the errors in each flight and with precise track recovery, post-flight correction may be attempted. A study is underway for a correction proce-